Soil pH in Europe

The JRC created a quantitative map of estimated soil pH values across Europe from a compilation of 12,333 soil pH measurements from 11 different sources, and using a geo-statistical framework based on Regression-Kriging. Fifty-four (54) auxiliary variables in the form of raster maps at 1km resolution were used to explain the differences in the distribution of soil pH_{CaCl2} and the kriged map of the residuals from the regression model was added. The goodness of fit of the regression model was satisfactory ($R^2_{adj} = 0.43$) and its residuals follow a Gaussian distribution. The lowest values correspond to the soils developed on acid rock (granites, quartzite's, sandstones, etc), while the higher values are related to the presence of calcareous sediments and basic rocks. The validation of the model shows that the model is quite accurate ($R^2_{adj} = 0.56$). This shows the validity of Regression-Kriging in the estimation of the distribution of soil properties when a large and adequately documented number of soil measurements are available.

There is no consistent or harmonized soil profile database in Europe which allows for the generation of an overview of pH values across Europe using digital soil mapping techniques. Therefore, an attempt was made to combine, harmonize and QA/QC check values from 11 available databases in order to create a quantitative map of estimated soil pH values across Europe. It is realized that these databases reflect biased sampling strategies, non-precise coordinates, different sampling times (e.g. especially sensitive on agricultural soils) and many other factors which influence the predicted result. However, these databases represent a snap shot of available data on soil pH currently available in the European Soil Data Centre. The major distribution of soil pH with a reported quantitative uncertainty is described in order to determine the extent of the risk of acidification across Europe.

Methodology

Soil Database creation: Eleven soil profile databases which are available in the European Soil Data Center (ESDAC) have been used. The top layer of each soil profile stored in the following datasets has been obtained:

- ICP-Forest (FSS),
- soil profiles from the ecopedological map of Italy,
- FOREGS (SALMINEN *et al.* 2007),
- Spade (HIEDERER *et al.* 2006),
- Soveur (NACHTERGAELE *et al.* 2002),
- WISE (BATJES 2002),
- Galicia (RODRIGUEZ LADO 2008),
- Danube-SIS (Bavaria, Slovenia and Bulgaria)
- Puglia Soil Database.

Data were projected to the INSPIRE complained Lambert Equal Area (LAEA) projection, if not already available in that projection. The measurement of pH in the different databases was performed in different solutions (H_20, KCl, $CaCl_2$). For each database there was an adjustment, if necessary, to report the pH in $CaCl_2$ solution.

The following linear pedo-transfer functions were generated based on values reported for topsoil sampling locations from the WISE global soil database:

[1] $pH_{CaCl2} = 0.9761 * pH_{H20} - 0.427$ ($R^2 = 0.92$, n=1997)
[2] $pH_{CaCl2} = 1.0572 * pH_{KCl} + 0.123$ ($R^2 = 0.90$, n =377)

The validity of the global dataset derived pedotransfer function (pH_{KCl}=0.87 pH_{H20}, R_2 =0.93) was tested by comparing it against the fit obtained from pH data measured in KCl and H_20 from the Galicia DB (pH_{KCl}=0.84 pH_{H20}, R_2 =0.75, n = 414); a good agreement was observed.

Duplicate detection: A duplicate soil sampling location is defined as a point which is within 1,000 m of another point. Some of the datasets used in the analysis have insufficient precision in their geo-location, allowing for false positives. Duplicate points were identified and clustered with a minimum distance of 1,000 m to obtain single independent regions. From the total dataset of 12,333 sampling points, 2,093 were within 1,000 m of a neighboring point, resulting in 847 clusters. Clustering of the duplicates occurred mainly in regions where denser sampling occurred (e.g. Italy had 571 duplicates out of 5,114 records) however even random sampling designs such as the 813 points extracted from the FOREGS DB contained two sampling locations within 1,000 m of neighboring records. The average standard deviation of adjusted pH_{CaCl2} of all 847 clusters was 0.39 with a maximum standard deviation of 2.54, whereas the average difference between the minimum/maximum pH_{CaCl2} at each cluster location was 0.6 with a maximum difference of 4.1 reached at sampling location in Galicia. Minimum was in both cases 0.0. Therefore one can specify the measurement/scale error for an analysis of ~0.5 unit pH_{CaCl2}.

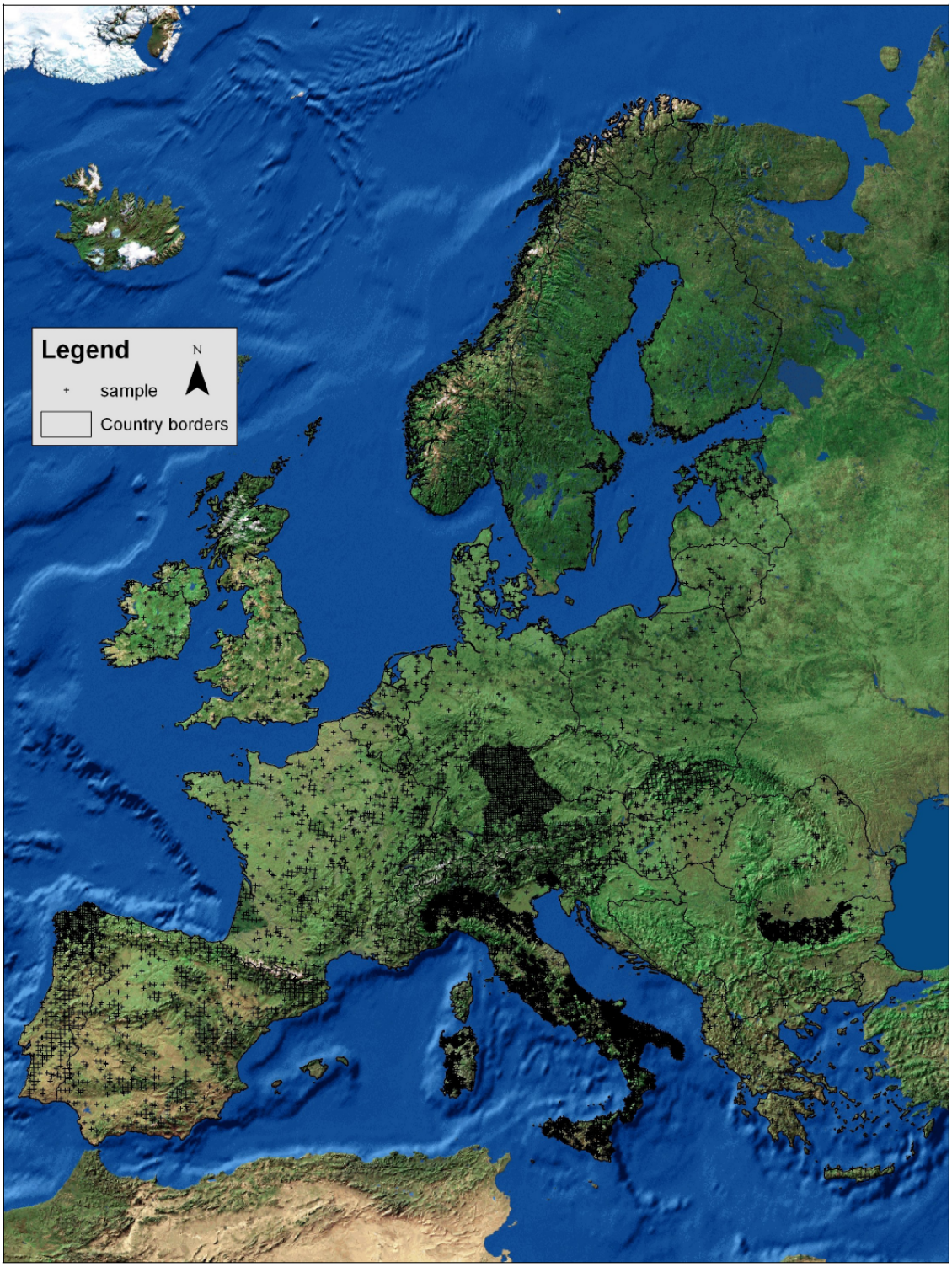

Fig. 1: Spatial distribution of soil sampling locations from the 11 different soil databases

Then it was checked if the chosen resolution was appropriate with respect to the pH_{CaCl2} point data.

Coarsest, finest and recommended cell sizes were determined following HENGL (2006) and were ~200 m, ~1km and ~4.7 km respectively. The 0.5 probability to meet the next point was reached at ~3 km (0.95 at 30 km), for 2 points at ~5 km (0.95 at 43 km), for all points at 1,000 km (0.95 probability at 2,700 km).

Geo-statistical mapping:

Regression-Kriging was used to estimate the pH_{CaCl2} values in soils of Europe. Firstly a linear regression model for the measured pH values was created against a number of auxiliary environmental variables and then the residuals of this regression model were interpolated by ordinary Kriging. The final map is an additive combination of both models. This technique allows to take into account the boundaries of some environmental features that can highly influence the distribution of the studied soil property in the final map of estimates, and thus to obtain more realistic predictions.

The original dataset of observations (12,333 records) was divided using a random sampling function into a "***model***" dataset, that includes the 80% of the samples and a "***validation***" dataset, containing the remaining 20% of the samples, that was using for validation of the model. The "model" points dataset was used to build the multiple linear regression model. The derived regression equation has than been applied on the standardized 1 km resolution 56 auxiliary raster grids. The results have been aggregated to 5 km resolution. The auxiliary variables are either directly influencing soil pH or serve as a proxy for a factor:

- *Topography*: The 1 km DEM was derived from the SRTM30 V2 dataset obtained from the JetPropulsion Laboratory. The SRTM DEM was used to derive a slope map, the Topographic Wetness Index (MOORE *et al.* 1991) and total incoming solar insolation (CONRAD 2001) using SAGA 2.0.

- *Geology*: the digital map of main geologic surface units in Europe was used (PAWLEWICZ *et al.* 2003). The original legend was reduced to 10 classes according to the genetic nature of each unit: (1) Granites, rhyolites and quartzites; (2) Paleozoic schists, phyllites, gneisses and andesites; (3) Shales and sandstones; (4) Mesozoic Ultramafic, basic phyllites, schists, limestones and evaporates; (5) Jurassic, Triassic and Cretaceous calcareous rocks; (6) Cenozoic serpentinites, gabros and sand deposits; (7) Tertiary basanites and andesites; (8) Neogene and Paleogene calcareous rocks; (9) Quaternary limestones and basaltic rocks; and (10) Other Ultramafic and undefined rocks.

- *EVI remote sensing images:* Monthly averaged MODIS images of the Enhanced Vegetation Index EVI at 1 km resolution for the period 01/01/2004 to 31/12/2006 were obtained from the MODIS Terra imagery at the Earth Observing System Data Gateway. A Principal Component Analysis was performed on the 19 complete mosaics and used the first five resulting components.

- *Image of Lights at Night:* The lights at night image for the year 2003 was obtained from the Defense Meteorological Satellite Program (http://www.ngdc.noaa.gov/dmsp/), which measures night-time light emanating from the earth's surface at 1 km resolution. This map is a proxy for urbanisation and is now increasingly used for quantitative estimation of global socioeconomic parameters as well as for human population mapping (SUTTON 1997, SUTTON *et al.* 1997, DOLL *et al.* 2000).

- *Distance to infrastructures*: The map of distances to roads, airports and utility lines was calculated using the distance operation in ILWIS and the GIS layers from the GISCO database of the European Commission.

- • *Cumulative Earthquake's magnitude*: The cumulative earthquake's magnitude map was calculated by using the 90,000 registered earthquakes in period 1973-1994. These measurements were recorded in the Global Seismology point database (http://earthquake.usgs.gov/eqcenter/). The logarithmic measure of the "size" of an earthquake was used and then the point map was rasterized to the 10 km grid by using the point density operation in ILWIS. This operation sums all earthquake magnitudes observed within a 10 km grid and gives a cumulative map of earthquake activity.

- *Land use:* The Corine Land Cover 2000 map of Europe generalized to a 1 km grid wa used. For Switzerland, the Corine Land Cover from 1990 was used since no updated information was available. The CLC1990 classes for this country were adjusted to those described in the CLC2000 and both datasets were merged together and aggregated to 1 km resolution. The original 44 classes were simplified to 8 classes: (1) urban infrastructures; (2) agriculture; (3) forest; (4) natural vegetation; (5) beaches; (6) ice bodies, (7) wetlands and (8) water bodies. Class 5 (beaches) disappeared in the process of upscaling from 100m to 1km. Additionally data from the Global Land Cover classification (FRITZ *et al.* 2003) has been used for areas where no Corine classification has been available.

- *Land forms:* The land forms were calculated by a modified method proposed by IWAHASHI & PIKE(2007). Basically it combines the topographic variables slope gradient, surface texture and local convexity to create 16 classes of landforms from steep to gentle landforms with fine/coarse texture and low/high convexity.

- *Climatic variables*: Mean annual temperature and accumulated precipitation maps were obtained from the very high resolution raster layers created by HIJMANS *et al.* (2005) on a global scale at 1 km grid resolution. The annual potential evapotranspiration (PET) was calculated from monthly temperature data using the THORNTHWAITE method (1948). Runoff was calculated as the difference between annual accumulated precipitation and annual potential evapotranspiration.

- *Alkalinity release rates due to the weathering of primary minerals in soils*: The release of alkalinity by weathering of primary minerals in soils was calculated using the *"Simple Mass Balance Method"* as described in RODRIGUEZ-LADO *et al.* (2007).

- *Atmospheric deposition of contaminants:* use was made of the estimated annual deposition and emission rates of cadmium, lead and mercury in Europe for year 2004 calculated within the European Monitoring Evaluation Programme (http://webdab.emep.int/). The original 50 km grids were downscaled to 1 km grids using ordinary kriging.

Non-soil surfaces such as water bodies (rivers, lakes, sea etc.) and permafrost areas were masked out. A consistent European wide water mask, indicating the percentage of water area inside a 1 km pixel, has been created based on the NASA SRTM V2 SWBDB dataset (RABUS *et al.* 2003), the CORINE land use classification, lakes contained in the GISCO data, base water reflection by the use of Image2000 dataset (DE JAGER *et al.* 2006), the GSHHS - Database (WESSEL & SMITH 1996), and the Global Lakes and Wetlands Database (LEHNER & DÖLL 2004).

Areas with permanent ice cover have been detected using the mean annual EVI derived from the

MODIS 1 km images obtained for the years 2003 and 2004. In this case, ice cover, water bodies and bare rock areas were detected based on a negative VI index. The total soil-cover area for these 26 countries was estimated to be 4,217,241 km2.

Each class within the categorical variables (geology, land use and land forms) was transformed to binary raster layers. Later all the auxiliary raster layers were standardized and finally converted to 54 Principal Component raster maps by Principal Component Analysis in ENVI v4.3in order to minimize co-linearity between variables. The kriging of the residuals from the linear model was done directly in 5 km blocks. In addition a measurement of the estimation errors associated to the kriging interpolation method was obtained.

Filtering the database of observations and building the regression model were performed in the statistical environment 'R v.2.6.0". The Principal Component Analysis of the standardized auxiliary variables was done using the image processing software ENVI. The raster linear model and the final Regression Kriging map were done in SAGA-GIS 2.0.

Results and discussion:

Descriptive statistics: The database used in this study is a compilation of samples collected in 11 different surveys (Fig. 2). There is a high variability of pH values across Europe, ranging from 0.09 to 1340. About 51 % of the samples present pH ≤ 10 while 41 % present values higher than 50 ppb. One can observe that the big survey campaigns across Europe (Soveur, Spade and FOREGS) present similar box-plot diagrams. However, the differences in pH are very evident when comparing regional campaigns on acidic soils like "Galicia" (parent materials mainly of granitic nature) and on calcareous soils like that in "Puglia" (mainly limestones). The higher pH measurements (pH =9) correspond to soils in Puglia (Italy) and high pH values (pH > 8) were also observed mainly in Bulgaria. Very low pH values (pH < 3) were observed in Bavaria (Germany), in the sandy soils from the "Landes" department in France, and in Belgium and UK.

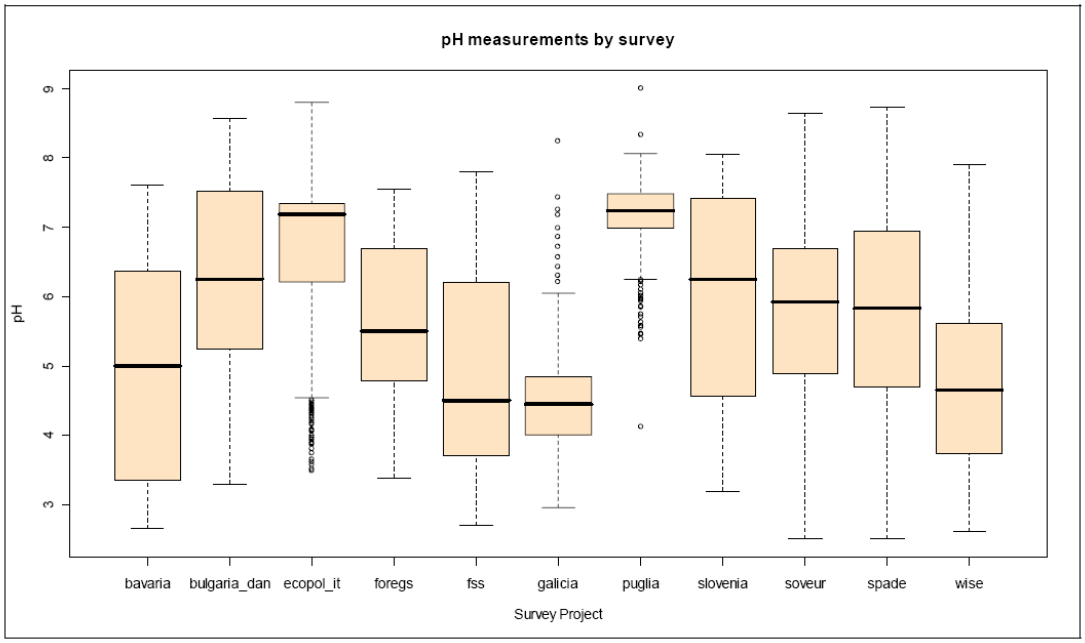

Fig. 2: Boxplot of the pH measurements by 11 different soil databases.

Geostatistics of the original data: The semi-variogram of the original data shows a moderate spatial dependency with a range of around 50-100 km (half of the total variance) and a slight linear trend up to 500 km (Fig. 3). Further analysis showed that this trend is due to a slight anisotropy in the east direction, whereas the north direction shows a periodic pattern. The semivariance shows two additional nested structures, which can be observed with a range of 600 km (reaching variance 1.6) and 800 km (reaching the total variance ~1.85). These two additional structures are due to anisotropy in the north–south direction, whereas the west-south direction shows only a prolonged trend as described before. Automated approaches fitting a semi variogram based on the range and total semivariance exist (see HENGL 2007). However,these would have missed the 50-100 km scale variation structures.

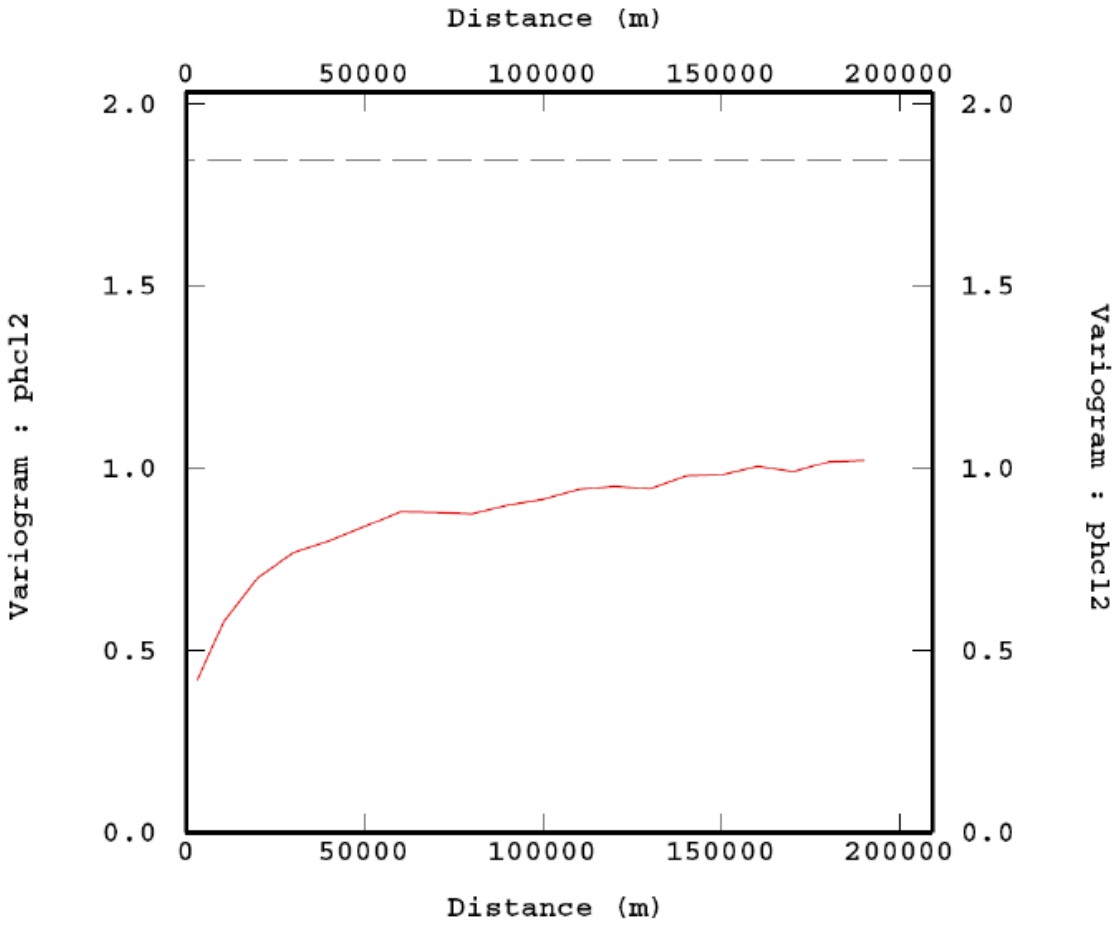

Fig. 3: Variogram of original pH_{CaCl2}

Linear Model results: The regression model obtained explains 43% of the variability (R^2_{adj}=0.433) and was significant at the $p<0.05$ level. Fifty one principal components contributed significantly ($p<0.05$) to the model (Tab. 1). The residuals of the regression model showed spatial structure and they were incorporated to the final model by ordinary-kriging using the software ISATIS V8.1 (GEOVARIANCES 2008). A spherical variogram was fitted to the observed semivariances with a

nugget of 0.55, a range of 20,000 and a sill of 1.22. The nugget/sill ratio (0.45) indicates that the residuals have a good spatial dependence.

Tab. 1: Regression coefficients for the multiple linear model.

VARIABLES	Estimate	VARIABLES	Estimate	VARIABLES	Estimate
(Intercept)	1.20E+03	[PCA18]	4.83E+01	[PCA36]	-7.49E-03
[PCA1]	2.28E-02	[PCA19]	1.26E+00	[PCA37]	8.70E-02
[PCA2]	2.69E-04	[PCA20]	-1.52E-01	[PCA38]	-1.16E-01
[PCA3]	9.64E-02	[PCA21]	-9.00E-01	[PCA39]	-9.67E-02
[PCA4]	-2.82E-01	[PCA22]	-5.82E-01	[PCA40]	2.88E-02
[PCA5]	-2.38E-01	[PCA23]	-4.20E+01	[PCA41]	6.24E-02
[PCA6]	2.89E-01	[PCA24]	4.21E-02	[PCA42]	6.13E-02
[PCA7]	4.17E-01	[PCA25]	-1.02E-01	[PCA43]	-8.06E-02
[PCA8]	-8.06E-01	[PCA26]	2.06E-02	[PCA45]	-1.14E-01
[PCA9]	-7.90E-01	[PCA27]	-5.87E-03	[PCA46]	4.67E-02
[PCA10]	-6.15E-01	[PCA28]	-3.65E-01	[PCA47]	-1.32E-02
[PCA11]	8.02E-02	[PCA29]	2.38E-01	[PCA48]	5.07E-02
[PCA12]	2.43E-01	[PCA30]	8.85E-03	[PCA50]	1.65E-02
[PCA13]	6.33E-01	[PCA31]	9.82E-02	[PCA51]	-9.83E-03
[PCA14]	5.59E-02	[PCA32]	-3.23E-03	[PCA53]	6.89E-03
[PCA15]	1.31E-01	[PCA33]	6.42E-02	[PCA54]	-2.77E-01
[PCA16]	4.30E-01	[PCA34]	-1.39E-01		
[PCA17]	-8.86E-01	[PCA35]	2.49E-01		

Tab. 1: Regression coefficients for the multiple linear model.

As suspected, the following map (Fig. 4) shows that the spatial distribution of soil pH is highly dependent on the nature of the parent material. One can observe low pH values in the granitic areas all over the Hesperic massif (Portugal and north of Spain), in the Vosges mountains, in the Pyrenees, and in the shallow soils from Scandinavia, mainly developed on acid materials. The higher pH values (pH > 7) are mainly present in the sedimentary areas of the Mediterranean countries (Spain south of France, Italy, Albania and Greece) because of the calcareous nature of the parent material. One can also observe differences due to land use patterns and large scale climatic differences (e.g. the Mediterranean area versus Scandinavia). These results might be useful in guiding further research - for example – as to why specific stream water catchments in the Czech republic showed differences in pH time series in periods of increasing acidic deposition (VESELY *et al.* 2002). According to computations 16.7% of the territory has pH values lower than 4.2 and only 1.9 % of the area present values of pH > 8. The higher pH estimates are located throughout all European countries, mainly located close to major cities, or in arid areas with intensive agriculture area (southeast of Spain) or Deltas. The distribution of pH values in relation to land use classes (Fig. 5) showed that forest soils have lower pH values, while agricultural and urban areas present the higher mean values probably due to liming and the influence of the dissolution of cement in buildings.

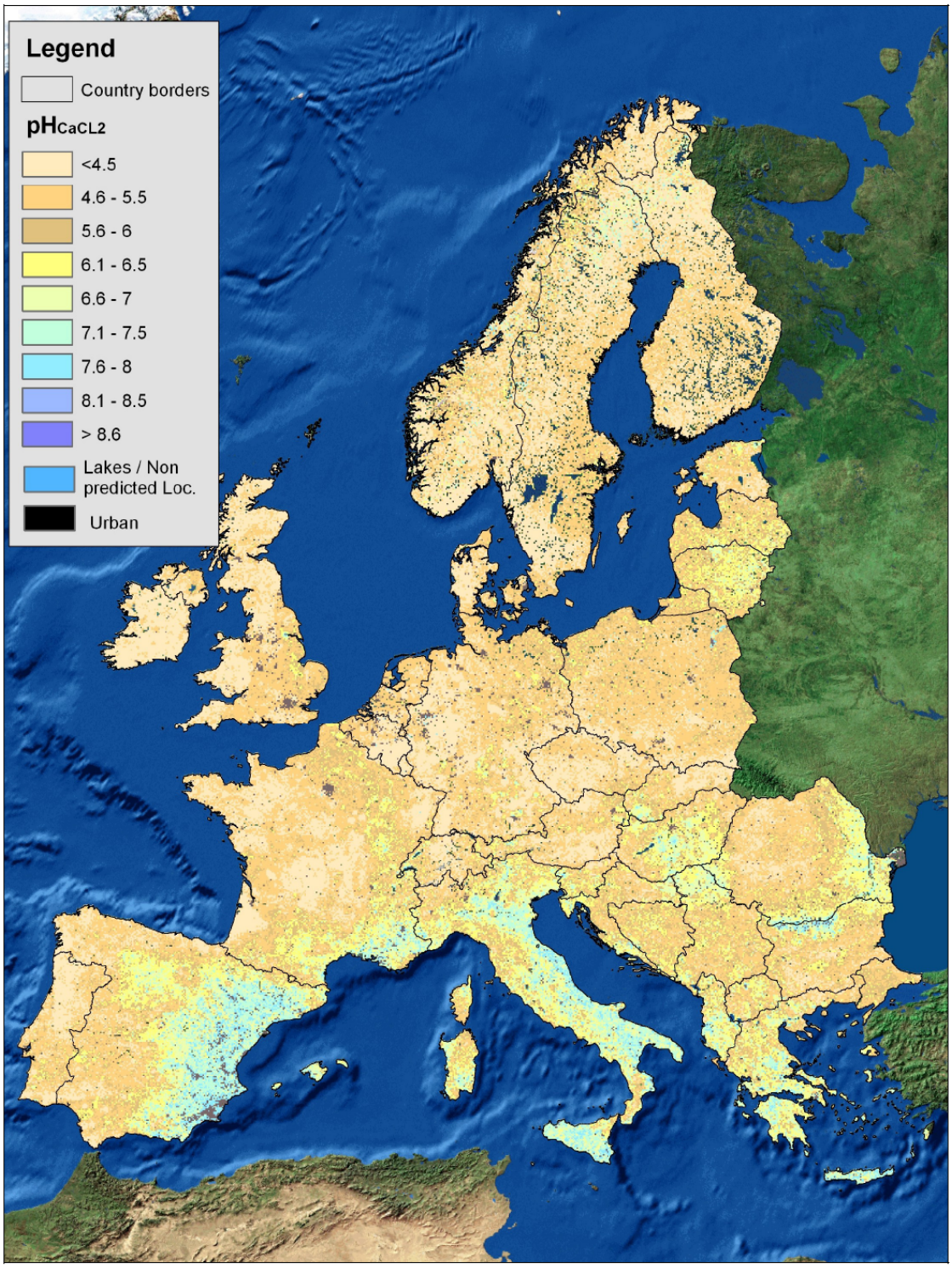

Fig. 4: Estimated values of pH_{CaCl2} for the EU27 MS and some adjacent countries.

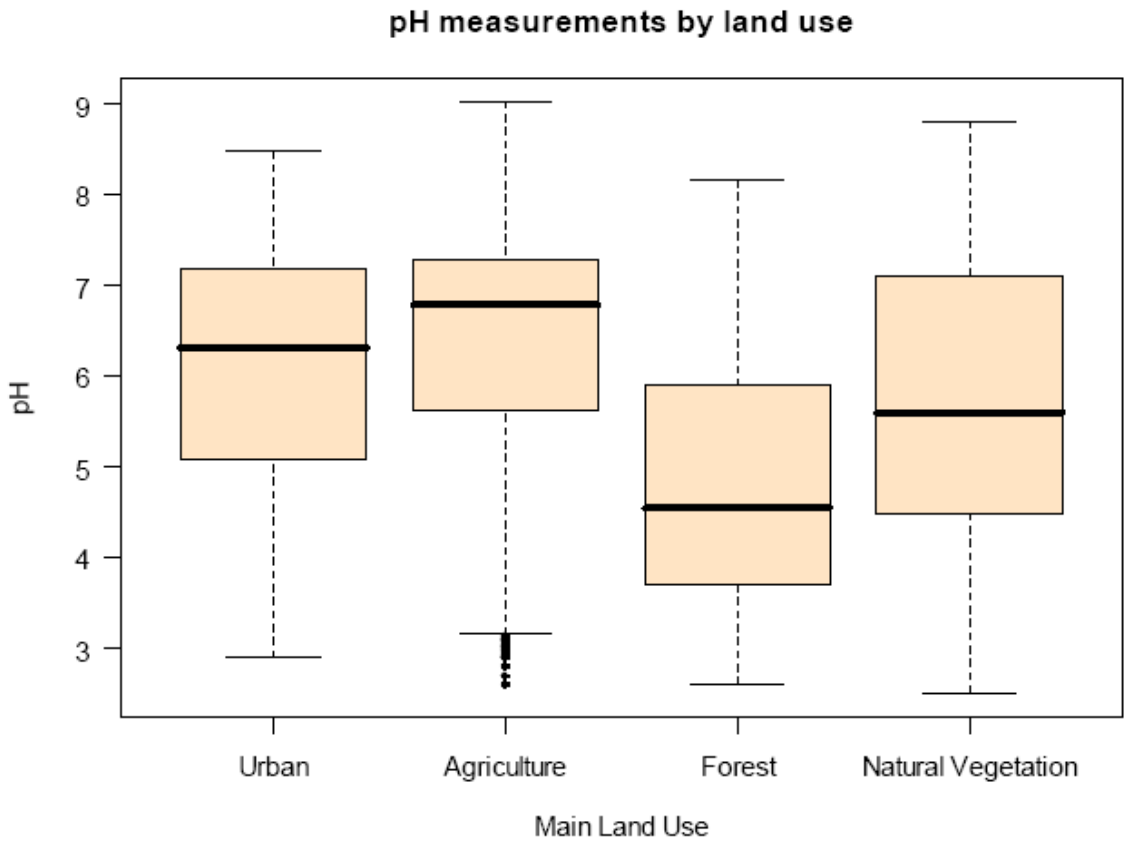

Fig. 5: Estimated pH_{CaCl2} boxplots for different major land uses

Validation: The accuracy of the model was assessed by comparing the pH measurements and their estimates in the 2,362 samples from the validation dataset. A linear regression was performed between both variables to check their relationship and a significant correlation between them was obtained (R^2_{adj}=0.56, a=0.05; Fig. 6). The equation of the regression model writes:

$$pH_{measured} = 1.34 + 0.779 * pH_{predicted}$$

Most of the samples fall within the limits of the 95% prediction bands. This relationship demonstrates that in general, the model slightly underestimates the real pH measurements. The Root Mean Square Error of the predictions is low (RMSE=0.9). A Student's t-test for paired samples ($p < 0.05$) shows that there are not significant differences between measurements and the predictions. The model does show a good fit in the prediction of soil pH values.

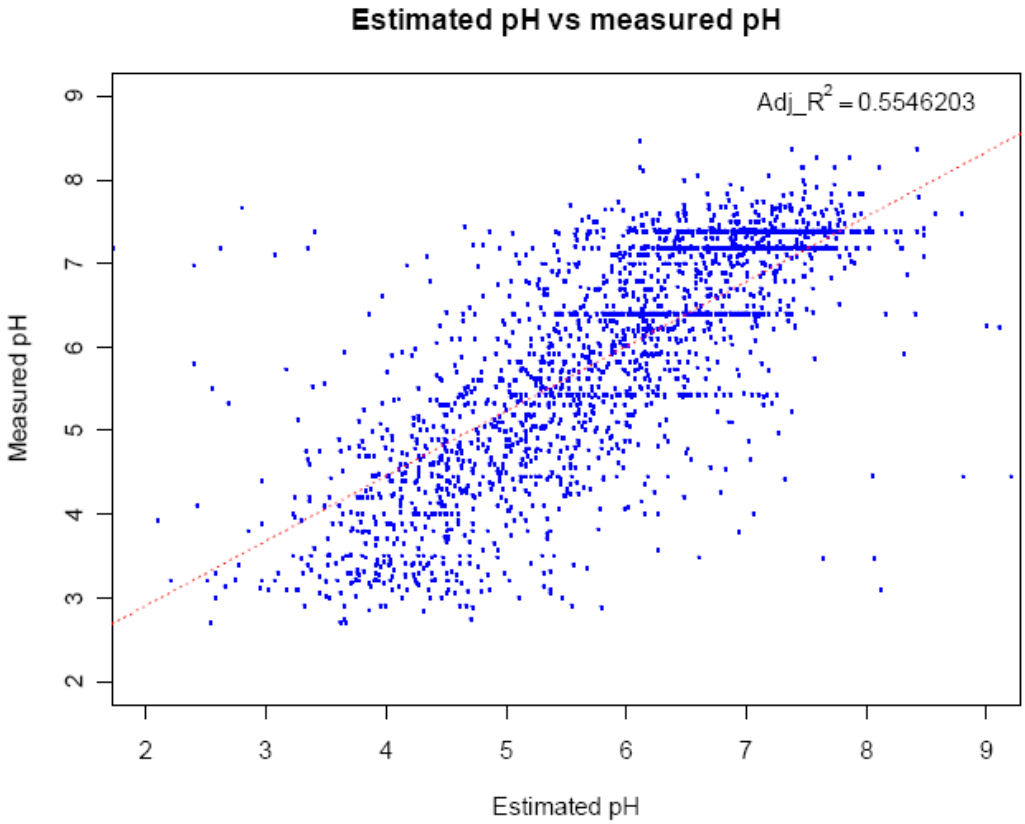

Fig. 6: Plot of measured vs. estimated pH in the validation dataset.

CONCLUSION

This study revealed that it was possible in a limited time and data frame to predict soil pH_{CaCl2}. This might serve as a first proxy to the sensitivity of soils to the process of acidification. The linear model was satisfactory and the residuals showed clear auto-correlation structure. If new data are available to be included in the DSM process, the procedure can be recomputed and uncertainties reduced. Any further assessment of sensitivity of soils to acidification has to take into account not only the pH but the soil organic matter content, soil texture and Al and Fe contents (KOPTSIK & ALEWELL 2007) as well as the sulphate sorption capacity of soils. One possible approach would be to generate a buffering capacity map using Digital soil mapping techniques, therefore providing an additional data set to the already existing critical load acidity maps (HETTELINGH *et al.* 1991, 1993, 1995). However, first impressions are that such DSM approaches would need a dedicated sampling campaign as well as standardized measurements for these kinds of parameters that are generally missing in the databases used in the study.

A further geo-statistical exercise would include simulations to predict probability density functions of the pH_{CaCl2} distribution. A disadvantage of this study is the lack of a temporal component. Most of the observations in the generated database contain no information on the time or timeframe of the sampling. If such information were available, maps for different times/time steps could be created, allowing results to be compared with changes in time as provided by e.g. de SCHRIJVER *et al.* (2006) or FÖLSTER *et al.* (2003).

REFERENCES

ALCAMO J., SHAW R. & L. HORDIJK (1990): The RAINS Model of Acidification. – Science and Strategies in Europe. Dordrecht, Netherlands: Kluwer Academic Publishers.

BATJES, N.H. (2002): Revised soil parameter estimates for the soil types of the world. – Soil Use and Management 18 (3):232–235.

CONRAD, O. (2001): Tools for (grid based) digital terrain analysis V1.0. – Program module for SAGA GIS 2.0, Göttingen.

DE SCHRIJVER, A., MERTENS, J., GEUDENS, G., STAELENS, J., CAMPFORTS, E., LUYSSAERT, S., DE TEMMERMAN, L., DE KEERSMAEKER, L., DE NEVE, S. & K. VERHEYEN (2006): Acidification of forested podzols in North Belgium during the period 1950-2000. – Science of the Total Environment, 361, 1-3, 189-195.

DE JAGER, A., RIMAVIČIŪTĖ, E. & P. HAASTRUP (2006): A Water Reference for Europe. – In: HAASTRUP, P. & WÜRTZ, J. (Eds.): Environmental Data Exchange Network for Inland Water (pp. 259-286, Elsevier.

DOLL, C.H., MULLER, J.P. & C.D. ELVIDGE (2000): Night-time Imagery as a Tool for Global Mapping of Socioeconomic Parameters and Greenhouse Gas Emissions. – AMBIO: A Journal of the Human Environment 29: 157-162.

FRITZ, S., BARTHOLOME, E., BELWARD, A., HARTLEY, A., STIBIG, H.-J. & H. EVA (2003): Harmonization, mosaicking, and production of the Global Land Cover 2000 database. – Joint Research Center (JRC), Ispra, Italy.

GEOVARIANCES (2008): ISATIS V8.1.1 Software for calculation of geostatistics.

HENGL, T. (2007): A Practical Guide to Geostatistical Mapping of Environmental Variables. – EUR 22904 EN Scientific and Technical Research series, Office for Official Publications of the European Communities, Luxemburg, 143 pp.

HENGL, T. (2006): Finding the right pixel size. – Computers & Geosciences 32 (9): 1283-1298.

HETTELINGH, J.P., DOWNING, R.J. & P.A.M. DE SMET (1993): Maps of critical loads, critical sulphur deposition and exceedances. – In: DOWNING, R.J., HETTELINGH, J.P. & P.A.M. DE SMET (Eds.): Calculation and mapping of critical loads in Europe. – Status report 1993. The Netherlands7 Coordination center for effects, RIVM; p. 6 – 18.

HETTELINGH, J.P, POSCH, M. & P.A.M. DE SMET (1995): Analysis of European maps. – In: POSCH, M, DE SMET, P.A.M., HETTELINGH, J.P. & R. DOWNING (Eds.): Calculation and mapping of critical thresholds in Europe. – Status report 1995. Bilthoven, The Netherlands7 Co-ordination Centre for Effects, National Institute of Public Health and the Environment; p. 5 – 22.

HETTELINGH, J.P., DOWNING, R.J. & P.A.M. DE SMET (1991): European critical loads maps. – In: HETTELINGH, J.P., DOWNING, R.J. & P.A.M. DE SMET (Eds.): Mapping critical loads for Europe. – CCE technical report 1. Bilthoven, the Netherlands7 Coordination Center for Effects, National Institute for Public Health and Environmental Protection; p. 5 – 30.

HIJMANS, R.J., CAMERON, S.E., PARRA, J.L., JONES, P.G. & A. JARVIS (2005): Very high resolution interpolated climate surfaces for global land areas. – International Journal of Climatology 25: 1965-

1978.

HIEDERER, R., JONES, R.J.A. & J. DAROUSSIN (2006): Soil Profile Analytical Database for Europe (SPADE): Reconstruction and Validation of the Measured Data (SPADE/M). – Geografisk Tidsskrift, Danish Journal of Geography 106(1): 71-85.

FÖLSTER, J., BISHOP, K., KRAM, P., KVARNAS, H. & A. WILANDER (2003): Time series of long-term annual fluxes in the streamwater of nine forest catchments from the Swedish environmental monitoring program (PMK 5). – The Science of The Total Environment, 310, Issues 1-3: 113-120.

IWAHASHI, J. & R.J. PIKE (2007): Automated classifications of topography from DEMs by an unsupervised nested-means algorithm and a three-part geometric signature, Geomorphology 86: 3-4 and 409-440.

INSAM, H. & A. PALOJÄRVI (1995): Effects of forest fertilization on nitrogen leaching and soil microbial properties in the Northern Calcareous Alps of Austria. – Plant and Soil, 168-169,1: 75-81.

KOPTSIK, G. & C. ALEWELL (2007): Sulphur behaviour in forest soils near the largest SO2 emitter in northern Europe. – Applied Geochemistry 22,(6): 1095-1104.

LEHNER, B. & P. DÖLL (2004): Development and validation of a global database of lakes,reservoirs and wetlands. – Journal of Hydrology 296: 1-22.

MOORE, I.D., GRAYSON, R.B. & A.R. LADSON (1991): Digital Terrain Modelling: A Review of Hydrological, Geomorphological and Biological Applications. – Hydrological Processes 5: 3-30.

NACHTERGAELE F.O., VAN LYNDEN, G.W.J. & N.H. BATJES (2002): Soil and terrain databases and their applications with special reference to physical soil degradation and soil vulnerability to pollution in Central and eastern Europe. – In: PAGLIAIA, M. (Ed.): Advances in GeoEcology 35. CATENA Verlag GMBH, Reiskrirchen.

NAVRÁTIL, T., KURZ, D., KRÁM, P., HOFMEISTER, J. & J. HRUSKA (2007): Acidification and recovery of soil at a heavily impacted forest catchment (Lysina, Czech Republic) – SAFE modeling and field results. – Ecological Modelling 205: 3-4 and 464-474.

ODEN, S. (1968): The acidification of air and precipitation and its consequences in the natural environment. – Ecological Committee Bulletin No. 1. Swedish Natural Science Research Council, Stockholm. Translations Consultants, Ltd. Arlington, Va.

PAWLEWICZ, M.J., STEINSHOUER, D.W. & D.L. GAUTIER (2003): Map Showing Geology, Oil and Gas Fields, and Geologic Provinces of Europe including Turkey.

RABUS, B., EINEDER, M., ROTH, A. & R. BAMLER (2003): The shuttle radar topography mission – a new class of digital elevation models acquired by spaceborne radar. – Photogrammetric Engineering and Remote Sensing 57: 241-262.

RASMUSSEN, P.E. & C.R. ROHDE (1989): Soil Acidification From Ammonium-Nitrogen Fertilization in Moldboard Plow and Stubble-Mulch Wheat-Fallow Tillage. – Soil Sci Soc Am J. 53: 119-122.

RODRIGUEZ LADO, L., HENGL, T. & H.I. REUTER (2008?): Heavy metals in European soils: a geostatistical analysis of the FOREGS Geochemical database. – Geoderma (in revision).

RODRIGUEZ LADO, L. (2008): personal communication.

RODRIGUEZ-LADO, L., MONTANARELLA, L. & F. MACÍAS (2007): Evaluation of the sensitivity of European soils to the deposition of acid compounds: Different approaches provide different results. – Water, Air and Soil Pollution 185: 293-303.

SALMINEN, R., BATISTA, M.J., BIDOVEC, M., DEMETRIADES, A., DE VIVO, B., DE VOS, W., DURIS, M., GILUCIS, A., GREGORAUSKIENE, V., HALAMIC, J., HEITZMANN, P., LIMA, A., JORDAN, G., KLAVER, G., KLEIN, P., LIS, J., LOCUTURA, J., MARSINA, K., MAZREKU, A., O'CONNOR, P.J., OLSSON, S.Å., OTTESEN, R.-T., PETERSELL, V., PLANT, J.A., REEDER, S., SALPETEUR, I., SANDSTRÖM, H., SIEWERS, U., STEENFELT, A. & T. TARVAINEN (2005): Geochemical Atlas of Europe. – Part 1/2 - Background Information, Methodology and Maps.

SCHEFFER, F., SCHACHTSCHABEL, P., BLUME, H.P., BRÜMMER, G., HARTGE, K.H., SCHWERTMANN, U., FISCHER, W. R., RENGER, M. & O. STREBEL (1992): Lehrbuch der Bodenkunde. – Enke, Stuttgart, 1-491.

SUTTON, P. (1997): Modeling population density with night-time satellite imagery and GIS. – Computers, Environment and Urban Systems 21: 227-244.

SUTTON, P., ROBERTS, D., ELVIDGE, C. & H. MEIJ (1997): A comparison of nighttime satellite imagery and population density for the continental United States. – Photogrammetric Engineering and Remote Sensing 63: 1303–1313.

THORNTHWAITE, C.E. (1948): An approach towards a rational classification of climate. – Geographical Review 38: 55-94.

ULRICH, B. (1981): Theoretische Betrachtungen des Ionenkreislaufs in Waldökosystemen. – Zeitschrift für Pflanzenernährung und Bodenkunde 144: 647-659.

ULRICH., B. (1983): Soil acidity and its relation to acid deposition. – In: ULRICH, B. & J. PANKRATH (Eds.): Effects of Accumulation of Air Pollutants in Forest Ecosystems. – Proc. Workshop,16-19 May, 1982, Gijttingen.Reidel, Dordrecht, The Netherladds, pp. 127 146.

VESELÝ, J., MAJER, V., & S.A. NORTON (2002): Heterogeneous response of central European streams to decreased acidic atmospheric deposition, Environmental Pollution 120(2): 275-281.

WESSEL, P. & W.H.F. SMITH (1996): A Global Self-consistent, Hierarchical, High-resolution Shoreline Database. – J. Geophys. Res. 101: 8741-8743.